Spatially Nonuniform Reaction Rates during Selective Oxidation on Gold

Fang Xu,[1] Robert J. Madix,[2] Cynthia M. Friend[1,2,*]

[1]Department of Chemistry and Chemical Biology, Harvard University, Cambridge, MA 02138, USA

[2]John A. Paulson School of Engineering and Applied Sciences, Harvard University, Cambridge, Massachusetts 02138, USA

KEYWORDS: In situ; selective oxidation of alcohols; gold; kinetic effect; STM

ABSTRACT: The nonuniform reactivity of adsorbed oxygen during the selective oxidation of methanol on Au(110)-(1×2) was demonstrated using *in situ* scanning tunneling microscopy (STM), establishing the importance of both atomic- and meso-scale structure in determining reaction kinetics. At coverages above 0.06 ML oxygen consumption occurs preferentially along [1$\bar{1}$0] direction, creating local regions completely devoid of oxygen between oxygen islands. The directionally specific reactivity is attributed to a combination of the weaker binding of oxygen atoms at chain termini and the release of surface strain induced by O bonding to Au. The generality of this phenomenon is illustrated by analogous, but kinetically contrasting behavior, for reaction of 2-propanol with oxygen covered Au(110)-(1×2). Even at low O coverages there are structurally related changes in the reactivity for the reaction with methanol. With decreasing O coverage: a slow reaction period is followed by a fast reaction period, the latter starting when oxygen coverage decreases to ~0.06 monolayer, independent of the initial coverage. This increase in reactivity is attributed to a sudden destabilization of the island structure. These results demonstrate that both local and mesocale structure can affect reactivity.

INTRODUCTION

Understanding the relationship between structure and reactivity is central to the prediction of chemical phenomena. In heterogeneous reactions, including catalysis, local structure and mesoscale ordering across a surface can potentially affect reactivity.[1-3] Usually, the structure during a reaction is dynamic and varies before and after the reaction.[4-5] Investigations of surface structure in real time is one of the few ways to identify active sites/phases. In this work, we use the selective oxidation of short-chain alcohols on gold surfaces as a prototype to study the dynamic structure during reaction.

Gold surfaces selectively oxidize short-chain alcohols below 350 K.[6-9] The first reaction step is transfer of the alcoholic proton to O adsorbed on the gold; the O serving as a Broensted base.[10] Subsequently, the alkoxide formed undergoes β-C-H bond scission. Thus, primary alcohols, including methanol and ethanol, first yield aldehydes, which subsequently couple with nearby alkoxides to form esters, e.g. methyl formate or ethyl acetate from methanol and ethanol respectively.[7] Ketones are formed from secondary alcohols, e.g. acetone from 2-propanol, through a similar mechanism.[6]

The selectivity for alcohol oxidation is generally highest at low oxygen coverages (θ_O) both for single crystal Au and on the catalytic surfaces,[9, 11-12] which is also the regime studied in this work. Specifically, the selectivity for methyl formate production from methanol oxidation on Au(110) was measured to be 100% for O coverages below 0.08 ML.[7] The ratio of O consumed to methyl formate produced is 1:1 in this coverage regime. The selectivity and reactivity for methanol is also higher at lower oxygen coverages on other gold surfaces, such as Au(111).[6, 12]

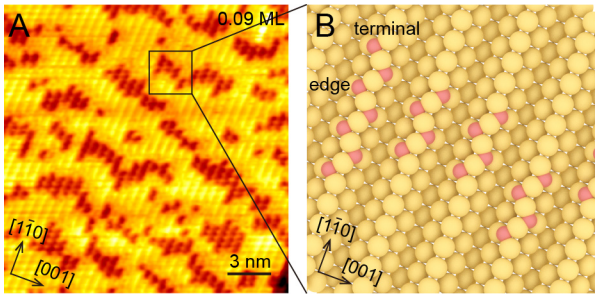

Figure 1. Structure of the oxygen chain groups on Au(110). (A) An STM image of the oxygen chain groups (dark) on Au(110) at room temperature. (θ_O = 0.09 ML) Image size: 25 × 25 nm^2; scanning conditions: 1.43 V, 0.1 nA. (B) A schematic of local structure of chain groups from (A) based on DFT calculations[13]. Yellow spheres are gold atoms; red spheres are oxygen atoms. Terminal and edge O atoms are labeled.

Oxygen atoms self-assemble on Au(110) forming short chains oriented along the [1$\bar{1}$0] direction and mesoscale chain groups in the [001] direction that span 1.6 nm (2 oxygen chains) and more, depending on the coverage of oxygen. Au(110) naturally reconstructs to Au(110)-(1×2) under ultrahigh vacuum conditions. Usually Au(110)-(1×2) surface is referred to as Au(110) in UHV studies. 1 monolayer is defined as one oxygen atom per gold atom on the top layer, i.e., four oxygen atoms in one Au(110)-(1×2) unit cell.[14] All oxygen atoms form zig-zag chains on the Au(110) surface at coverages up to 0.25 ML by occupying pseudo 3-fold coordination sites on the alternative side of the Au ridge.[7, 13] At θ_O ~ 0.1 ML, the oxygen chains usually are self-limited in length along the row direction and appear side by side with some overlapping of neighboring chain

groups, shown as chain ribbons on the surface (Fig. 1A). Atomically resolved STM indicates the zig-zag structure is maintained within the chain groups (a schematic in Fig. 1B).[13] The length of the chain groups along the [001] direction increases with θ_O, and eventually covers the whole terrace.

Binding of O leads to changes in the Au-Au bond in the vicinity of the adsorbed O. For example, Au bound to 2 O atoms is displaced outward from the surface by 0.6 Å.[13] There is also a small lattice expansion (~7% increase) in the $[1\bar{1}0]$ direction.[13] These structural distortions create strain within Au atoms along the $[1\bar{1}0]$ direction, leading to the short length of O chains. Specifically, the predominant O chain at a coverage of ~0.05 ML is composed of 3 – 7 oxygen atoms, i.e. 0.8 – 2.0 nm in length.[7, 15] Interestingly, the oxygen chains form a very similar structure at low coverage on Pt(110)-(1×2). Theoretical calculations indicate that the elastic relaxation along the $[1\bar{1}0]$ direction in the top layers influences the bulk layers, which is responsible for the weak attractive interactions between O chains[16]. Because of the similarity in structure, the influence from the bulk is anticipated to also occur on oxygen covered Au(110)-(1×2) surface. At θ_O = 0.09 ML the [001]-oriented O chain groups extend across as many as 30 Au ridges.

Herein, the dynamic oxygen structure was captured during methanol oxidation on Au(110)-(1×2)-O at low oxygen coverage (θ_O < 0.1 ML) using *in situ* scanning tunneling microscopy (STM) at room temperature. The experiments show that oxygen does not re-distribute on the time scale of its removal, leaving a non-uniform distribution with large patches of Au as the reaction proceeds. The anisotropic phenomenon is ascribed to the higher activity of terminal O atoms and the release of strain within Au due to oxygen removal. The generality of this phenomenon was demonstrated by investigation of 2-propanol oxidation on Au(110)-(1×2)-O. The initial θ_O influences the fast and slow reaction periods. The results demonstrate that both local and mesoscale structure of the oxygen group chains with the gold substrates play a role in activity and that the active phase is only present during alcohol oxidation on gold surfaces.

EXPERIMENTAL METHODS

All experiments in this work were done in a commercialized Omicron VT Beam Deflection AFM/STM housed in an ultra-high vacuum (UHV) chamber with a preparation chamber at room temperature. The background pressure was 2×10^{-10} mbar. A Au(110) single crystal sample (Princeton Scientific Corp.) was cleaned by 15 min sputtering – room temperature ozone treatment – 10 min annealing cycles in the preparation chamber (Ar, Airgas east, ultra-high purity grade; ~2×10^{-7} mbar O_3 inside the UHV chamber, 61 g/Nm^3 outside flow circuit; ~900 K annealing in UHV). Ozone was generated by a commercial ozone generator (ozone engineering, LG-7) with a concentration monitor (Teledyne Instruments, Model 454H). A cut Pt-Ir tip was used for scanning. The *in situ* measurements were conducted when alcohol vapors were dosed through a direct dosing tube within 2 cm to the sample while scanning. As discussed in our previous study,[15] the effective pressure under the STM tip during *in situ* measurement is estimated to be slightly higher than the readings of an ion gauge equipped in the chamber, which is reported in this work.

RESULTS AND DISCUSSION

Methanol and 2-propanol both react with adsorbed oxygen on Au(110) to yield selective oxidation products (Fig. 2). As noted above both alcohols react with adsorbed O, yielding the respective alkoxy intermediates.[7] At room temperature, methoxy and 2-propoxy react rapidly to produce methyl formate[7] and acetone.[17] Oxygen is removed as water. All species have a surface lifetime less than 3×10^{-4} s at 300 K (Table S1, calculation details in SI) – faster than the time to scan one pixel (4×10^{-4} s), and are, therefore not imaged in STM. Hence, the reaction removes surface oxygen, ultimately producing a clean Au(110) surface at room temperature (Fig. 2).

The spatial distribution of reaction with methanol and 2-propanol were monitored by imaging changes in the distribution and coverage of adsorbed O using *in situ* STM. Oxygen atoms have limited mobility on Au(110) at 300 K, so that neither the overall oxygen coverage nor the distribution of oxygen atoms change in the absence of reaction (Fig, S1). Furthermore, the scanning conditions used in this work do not induce oxygen mobility. While water, one of the reaction products, does induce mobility of adsorbed O under these same conditions, it does not change the overall distribution.[15] Hence, changes in O atom distribution provide a picture of the spatial distribution of alcohol oxidation and O removal.

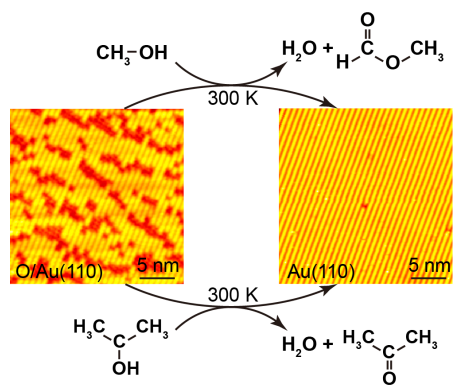

Figure 2. Schematic of the selective oxidation reactions of methanol and isopropanol in this work. The STM images correspond to O-covered Au(110) (left) and clean Au(110) (right). Scanning conditions 1.43 V, 0.1 nA.

Imaging of an oxygen pre-covered Au(110) surface during exposure to methanol at room temperature provides evidence of non-uniform removal of adsorbed oxygen atoms under steady-state conditions (Fig. 3). Once removal of O chain commences, adjacent areas along the $[1\bar{1}0]$ direction become devoid of oxygen (dashed black box in Fig. 3B to 3D). The growth rate of the cleared Au area increases non-linearly with time and preferentially along the $[1\bar{1}0]$ direction: the average O consumption rate in length and width from Fig. 3C to 3D is ~0.2 nm/min and ~0.1 nm/min respectively. Simultaneously, the average width ([001]) of O chain groups is diminished (Fig. S2).

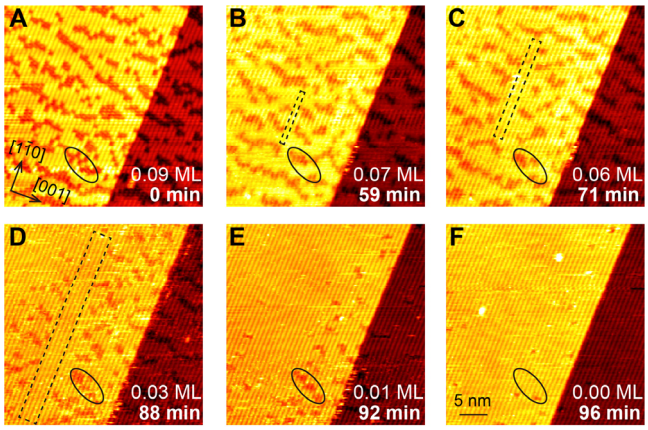

Figure 3. *In situ* STM of methanol reacting with O covered Au(110) at room temperature ($P_{methanol} = 9\times10^{-9}$ mbar; $\theta_O = 0.09$ ML). Oxygen atoms are imaged as dark features. Oxygen coverage and methanol exposure time are indicated in each panel. The development of the region defined by the dashed black box shows the preferred reaction direction along the [1$\bar{1}$0] direction. Black circles were drawn as landmarks. The same area was recorded of a size of 36×36 nm^2; scanning conditions: 1.43 V, 0.1 nA.

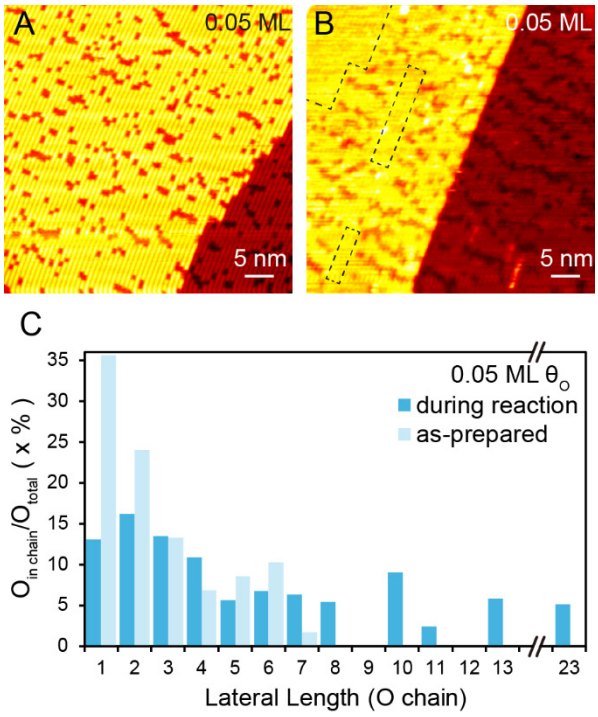

Figure 4. Distributions of oxygen chains in lateral direction (A) on an as-prepared Au(110) surface ($\theta_O = 0.05$ ML), and (B) during methanol oxidation on Au(110) ($\theta_O = 0.05$ ML) at room temperature. Gold areas from non-uniform O consumption were highlighted in black dashed boxes. (C) Statistics of lateral length of O chain groups in (A) and (B). The count of O atoms in a chain group is weighted as percentage of total O atoms in the image. Both STM images are of 50×50 nm^2. Scanning conditions: 1.43 – 1.8 V; 0.1 nA.

The non-uniform O removal is ascribed to two factors: (1) Terminal O atoms are more weakly bound,[15] and are, therefore, more reactive. Removal of a terminal O atom exposes yet another terminal O, leading to preferred reaction along the [1$\bar{1}$0] direction. (2) Binding to O induces strain along the [1$\bar{1}$0] direction and perturbations in the top layers, which is responsible for the attractive interaction between O chains.[16] Strain within the underlying Au atoms is released due to the O removal in adjacent areas, resulting in destabilization of the O chains in an adjacent area. Therefore, clean Au patches grow two dimensionally as the reaction proceeds.

The distribution of oxygen chains during methanol reaction differs from that on an as-prepared Au(110) substrate at the same O coverage. In the latter case, O chains are evenly distributed across the surface (Fig. 4A, $\theta_O = 0.05$ ML). At this low coverage, ~35% of the O atoms are presented in a chain without neighbors; the rest form chain groups along the [001] direction, with the largest group made of 7 O chains (Fig. 4C, "as-prepared" plot). However, at the same θ_O during reaction with methanol (initial $\theta_O = 0.09$ ML) the surface contains large Au patches (dashed black box in Fig. 4B) and disproportionally much larger O chain groups, with the largest group consisting of 23 O chains (Fig. 4C, "during reaction" plot). Clearly, the removal of O atoms on Au(110) by methanol at room temperature leads to kinetically trapped structures that cannot re-distribute on the timescale of O removal, which allows the active site(s) for the reaction at chain termini to be mapped.

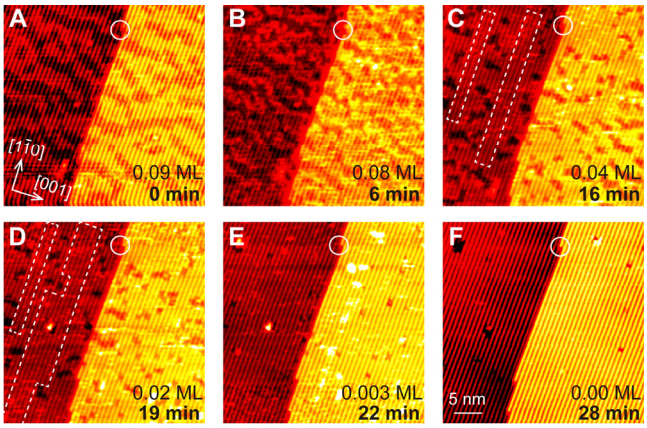

Figure 5. *In situ* STM of 2-propanol reacting with O covered Au(110) at room temperature ($P_{2\text{-propanol}} = 3.3\times10^{-10}$ mbar; $\theta_O = 0.09$ ML). Oxygen coverage and dosing time are indicated in each panel. Dashed white boxes show the preferred reaction along the [1$\bar{1}$0] direction. White circles indicate a landmark showing the same area was recorded of a size of 36×36 nm^2; scanning conditions: 1.2 V, 0.09 nA.

To explore further the generality of the anisotropic removal of O, we conducted *in situ* experiments using 2-propanol on an oxygen covered Au(110) surface (Fig. 5). The evolution of the surface oxygen structure is very similar to that seen during the reaction with methanol; the lateral interactions among oxygen chains break down and large patches of Au appear (Fig. 5C, 5D): the general pattern of reactivity remains. The non-uniform O structure during the reaction with short-chain alcohols is thus attributed to the characteristics of the oxygen covered Au(110) surface.

Quantitative analysis of *in situ* STM indicates that the reaction with methanol is divided into an induction period followed by slow and fast reaction periods and that the acceleration of the reaction rate occurs for the same O coverage (~0.06 ML) for the two different initial O coverages (Fig. 6A). While the acceleration in rate occurs at the same O coverage for the two different initial coverages, the absolute rate is slightly different (Fig. 6A).

Examination of STM images taken during reaction of methanol when the O coverage reaches ~0.06 ML for the two different initial coverages shows that the O distribution and the rates of reaction are slightly different for the two cases (Fig. 6B, 6C). Furthermore, these structures are different than an equilibrated structure (Fig. 4A). In other words, the exact rate of methanol reaction depends on the O distribution and during reaction, the O distribution does not reorganize to uniformly cover the surface on the time scale of the reaction.

Analysis of STM data further shows that the O chains are slowly consumed by reaction with methanol after a short induction period, eventually breaking up some two-dimensional O chain groups into smaller islands, and slightly shortening the O chain length within chain groups (Fig.S2 and S3). At θ_O ~0.06 ML (Fig. 6B, 6C), when the fast reaction period ensues with zero order kinetics (Fig. 6A), reaction with terminal O atoms dominates the reaction. As noted above, the initial oxygen coverage has an influence on the nonuniform oxygen consumption. The Au(110) surface with an initial O coverage of 0.07 ML has narrower oxygen chain groups along the [001] lateral direction, i.e., within Au rows, compared to the surface with an oxygen coverage of 0.09 ML. The breakdown of the O-chain groups with a smaller initial O coverage leads to a surface with more isolated O chains and less obvious large Au areas, as shown in Fig. 6B and 6C.

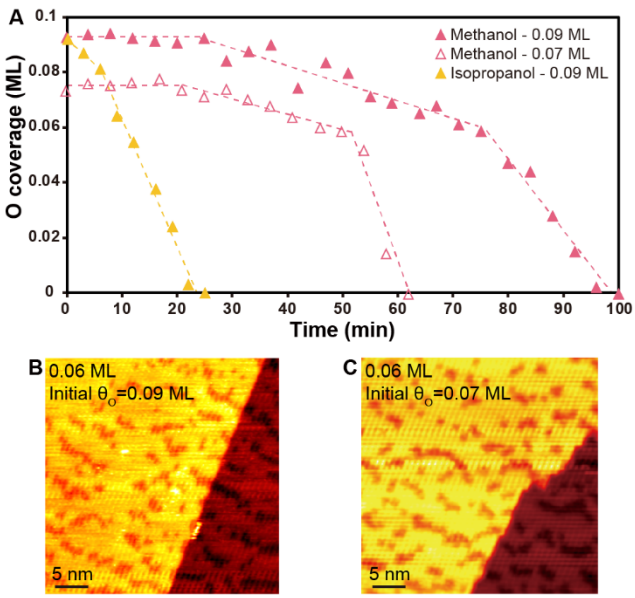

Figure 6. (A) Comparison of oxygen consumption by methanol with two initial oxygen coverages and isopropanol on Au(110) surface at room temperature ($P_{methanol} = 9\times10^{-10}$ mbar, $\theta_O = 0.09$ ML and 0.07 ML; $P_{isopropanol} = 3.3\times10^{-10}$ mbar, $\theta_O = 0.09$ ML). Trendlines are plotted in the induction, slow, and fast reaction periods. (B) and (C) correspond to surfaces at the onset of the fast reaction period during the reaction with methanol in (A). Both images are of 36×36 nm^2. Scanning conditions: 1.43 V; 0.1 nA.

The number of periphery oxygen atoms, i.e., oxygen atoms on the boundary of 2D O chain groups including all terminal and edge O atoms, is linearly correlated with the reaction rate during the slow reaction, because the reaction rate (O removal rate) is constant if normalized to the total periphery of oxygen chain groups (Fig. 7 "rate/p" plots). In accord, both the number of terminal and edge sites decreases slowly as the reaction proceeds (Fig. 7 "terminal O" plots). Since the terminal O atoms are highly actively consumed, this observation agrees with the conclusion that the terminal O atoms are active on Au(110).[15] At the onset of the rapid reaction the number of sites on the periphery suddenly decreases.

Our observation agrees well with the literature that oxygen at periphery sites has higher activity. Oxygen atoms tend to form chains/chain groups on a variety of (110) terminated transition metal surfaces, such as Cu(110),[18] Ag(110),[19] Rh(110),[20] Ni(110),[21] and Pd(110).[22] All but Rh(110) incorporate added metal atoms into the O chains to form metal-oxygen-metal bonds. These chains lie in the troughs along the [1$\bar{1}$0] direction. The chains react with CO,[19-20, 23-24] water,[25-27] methanol,[28-31] formic acid,[32] CO_2,[33] H_2S,[34-35] ammonia,[21] and benzotriazole.[36] Generally speaking, despite nuances in the structure of the oxygen chains, oxygen atoms on the periphery of chain groups are all reactive, with oxygen atoms on the terminal sites of the chains ([1$\bar{1}$0] ends) being more reactive than those on the side of chains.[18-19, 23, 26, 29, 32-33] Defect sites[18] and the reaction temperature[18, 24, 26] also play an important role. Further, when oxygen forms isotropic 2D islands on the (111) terminated surfaces, the reaction rate is proportional to the periphery of the oxygen islands.[37,38]

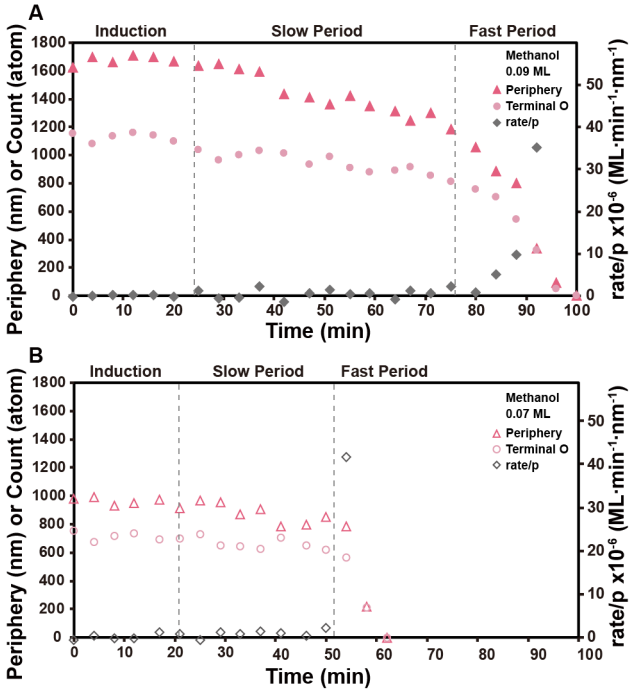

Figure 7. Decrease of periphery of O chain groups (the total length of O peripheral atoms in the unit of nm), consumption of terminal O atoms and ratio of reaction rate to the periphery (rate/p) during selective oxidation of methanol at room temperature. ($P_{methanol} = 9\times10^{-9}$ mbar; initial $\theta_O = 0.09$ and 0.07 ML) Induction, slow and fast reaction periods were separated by dash lines. Measurements of "0.09 ML" are based on an area of 43 × 43 nm^2; the other is based on an area of 36 × 36 nm^2. Calculation methods were described in detail in SI.

The origin of the transition from slow to faster consumption of the adsorbed O by methanol can be attributed to a decrease in the stability of the adsorbed O as the islands shrink to a size where the strain energies that contribute to their stabilization are diminished. The onset of the fast reaction correlates with breakup of the islands into smaller entities, as evidenced by the

sudden decrease in the number of terminal sites within the island structure (Fig. 7). Evidently, as the dimension of the island along the [1$\bar{1}$0] direction decreases, it reaches a limit where the cohesive energy that stabilizes the island decreases, leading to disintegration of the islands and more rapid reaction due to the lower stability of the adsorbed O.

The initial θ_O has an influence on both reaction regimes: 0.02 ML less initial θ_O leads to a shortening of the slow reaction period by 21 min, commensurate with the need to remove more adsorbed O prior to the onset of the faster reaction at ~0.06 ML O; and a 13 min reduction in the fast reaction period (Fig.4). The difference in rate in the fast reaction region observed for the two initial O coverages is attributed to the difference in structures descendant from the original coverage. An initial coverage of 0.07 ML contains more isolated O chains (Fig. 6B,C, Fig. S4, S5); the higher initial θ_O leads to a longer lateral width of O chain groups on the as-prepared surfaces.

The reaction of isopropanol with adsorbed O exhibits qualitatively similar behavior as methanol in that there is a slow reaction period followed by a fast reaction regime (Fig. 6A); however, the slow reaction period is shorter reflecting a faster reaction overall for isopropanol compared to methanol. Nevertheless, the evolution of the nonuniform O distribution is observed for isopropanol (Fig. 5), analogous to methanol. This general trend suggests that spatially non-uniform reaction is general for the oxidation of alcohols even if the absolute rate is different.

The higher reactivity of isopropanol is in agreement with previous studies which show dramatic difference between the reactivity of methanol and ethanol on O-precovered Au(110).[7] This dependence on the molecular structure can be attributed to the difference in elementary steps and the heterolytic O-H bond energies (gas phase acidities) of isopropanol when compared to methanol. In essence, since the reaction with the adsorbed O is a proton-exchange process with the alcohol, a lower activation barrier exists for the reaction with the larger alcohols. This lower barrier apparently compensates for the stability of the adsorbed O induced by the 2D cohesive energy of the oxygen layer induced by the lateral strain. Additionally, larger alcohols have stronger van der Waals interactions with the surface,[17] which lead to a longer surface lifetime that promotes activity.

CONCLUSIONS

In summary, non-uniform inhomogeneous consumption of oxygen atoms/chains occurs preferentially along the [1$\bar{1}$0] direction. The phenomenon is ascribed to high activity of terminal O atoms and the strain release of underlying Au atoms due to oxygen removal. Methanol exhibits slow and fast reaction periods that correlate with O coverage. The fact that the nonuniform distribution of O only exists during reaction also indicates that a metastable surface structure forms under reaction conditions. Once θ_O decreases to ~0.06 ML the rate of reaction increases dramatically and proceeds with apparent zero order kinetics. The onset of this higher reactivity correlates with disintegration of the island structure of the adsorbed oxygen.

These results demonstrate that both atomic-scale and mesoscale structures can develop during reaction to influence the reactivity in heterogenous systems. Accordingly, the rates can be non-uniform and also potentially depend on the overall spatial extent of the reactive intermediates on the surface. Dynamic and metastable surface structures may form during the reaction on a time scale faster than its reorganization into its most energetically favorable state, and, in turn, alter the rate.

These concepts may be relevant to nanoparticle metal catalysts as well. Specifically, the reactivity of O adsorbed on nanoparticles could be significantly affected, particularly if the terrace width on the surfaces were sufficiently small to prevent the formation of island structures stabilized by adsorbate-induced strain. The results are meaningful in understanding, designing and optimizing gold-based catalysts for selective oxidation.

ASSOCIATED CONTENT

Supporting Information. Supporting results, calculation methods of terminal and edge O, calculations of thermodynamic and kinetic properties of adsorbates, and corresponding STM movies of Fig. 3 and Fig. 5 are included in the supporting information. This material is available free of charge via the Internet at http://pubs.acs.org.

AUTHOR INFORMATION

Corresponding Author

* The corresponding author is Prof. Cynthia M. Friend, who can be reached at friend@fas.harvard.edu.

ACKNOWLEDGMENT

This work was financially supported as part of the Integrated Mesoscale Architectures for Sustainable Catalysis (IMASC), which is an Energy Frontier Research Center (EFRC) funded by the US Department of Energy (DOE), Office of Science, Basic Energy Sciences under award no. DE-SC0012573.
We would also like to thank Dr. Christian Reece and Mr. Christopher R. O'Connor for proof reading the article.

REFERENCES

(1) Fujita, T.; Guan, P.; McKenna, K.; Lang, X.; Hirata, A.; Zhang, L.; Tokunaga, T.; Arai, S.; Yamamoto, Y.; Tanaka, N.; Ishikawa, Y.; Asao, N.; Yamamoto, Y.; Erlebacher, J.; Chen, M. *Nat. Mater.* **2012**, *11*, 775-780.
(2) Eren, B.; Lichtenstein, L.; Wu, C. H.; Bluhm, H.; Somorjai, G. A.; Salmeron, M. *J. Phys. Chem. C* **2015**, *119*, 14669-14674.
(3) Paszti, Z.; Hakkel, O.; Keszthelyi, T.; Berko, A.; Balazs, N.; Bako, I.; Guczi, L. *Langmuir* **2010**, *26*, 16312-16324.
(4) Zhang, S. R.; Nguyen, L.; Zhu, Y.; Zhan, S. H.; Tsung, C. K.; Tao, F. *Acc. Chem. Res.* **2013**, *46*, 1731-1739.
(5) Zugic, B.; Wang, L.; Heine, C.; Zakharov, D. N.; Lechner, B. A. J.; Stach, E. A.; Biener, J.; Salmeron, M.; Madix, R. J.; Friend, C. M. *Nat. Mater.* **2016**, *16*, 558-564.
(6) Gong, J.; Flaherty, D. W.; Yan, T.; Mullins, C. B. *ChemPhysChem* **2008**, *9*, 2461-2466.
(7) Hiebel, F.; Karakalos, S.; Xu, Y.; Friend, C. M.; Madix, R. J. *Top. Catal.* **2017**, *61*, 299-307.
(8) Xu, Y.; Chen, W.; Kaxiras, E.; Friend, C. M., Madix, R. J. *J. Phys. Chem. B*, **2018**, *122*, 555-560.
(9) Gong, J.; Mullins, C. B. *Acc. Chem. Res.* **2009**, *42*, 1063-1073.
(10) Outka, D. A.; Madix, R. J. *J. Am. Chem. Soc.* **1987**, *109*, 1708-1714.
(11) Yan, T.; Gong, J.; Mullins, C. B. *J. Am. Chem. Soc.* **2009**, *131*, 16189-16194.
(12) Xu, B.; Liu, X.; Haubrich, J.; Madix, R. J.; Friend, C. M. *Angew. Chem., Int. Ed.* **2009**, *48*, 4206-4209.
(13) Hiebel, F.; Montemore, M. M.; Kaxiras, E.; Friend, C. M. *Surf. Sci.* **2016**, *650*, 5-10.
(14) Gottfried, J. M.; Schmidt, K. J.; Schroeder, S. L. M.; Christmann, K. *Surf. Sci.* **2003**, *525*, 197-206.
(15) Xu, F.; Fampiou, I.; O'Connor, C. R.; Karakalos, S.; Hiebel, F.; Kaxiras, E.; Madix, R. J.; Friend, C. M. *Phys. Chem. Chem. Phys.* **2018**, *20*, 2196-2204.

(16) Helveg, S.; Li, W. X.; Bartelt, N. C.; Horch, S.; Laegsgaard, E.; Hammer, B.; Besenbacher, F. *Phys. Rev. Lett.* **2007**, *98*, 4.
(17) Karakalos, S.; Xu, Y.; Cheenicode Kabeer, F.; Chen, W.; Rodríguez-Reyes, J. C. F.; Tkatchenko, A.; Kaxiras, E.; Madix R. J.; Friend, C. M. *J. Am. Chem. Soc.*, **2016**, *138*, 15243-15250.
(18) Crew, W. W.; Madix, R. J. *Surf. Sci.* **1996**, *349*, 275-293.
(19) Nakagoe, O.; Watanabe, K.; Takagi, N.; Matsumoto, Y. *J. Phys. Chem. B* **2005**, *109*, 14536-14543.
(20) Leibsle, F. M.; Murray, P. W.; Francis, S. M.; Thornton, G.; Bowker, M. *Nature* **1993**, *363*, 706-709.
(21) Ruan, L.; Stensgaard, I.; Lægsgaard, E.; Besenbacher, F. *Surf. Sci.* **1994**, *314*, L873-L878.
(22) Tanaka, H.; Yoshinobu, J.; Kawai, M. *Surf. Sci.* **1995**, *327*, L505-L509.
(23) Crew, W. W.; Madix, R. J. *Surf. Sci.* **1994**, *319*, L34-L40.
(24) Hartmann, N.; Madix, R. J. *Surf. Sci.* **2002**, *516*, 230-236.
(25) Savio, L.; Smerieri, M.; Vattuone, L.; Gussoni, A.; Tassistro, C.; Rocca, M. *Phys. Rev. B* **2006**, *74*, 6.
(26) Bobrov, K.; Guillemot, L. *Surf. Sci.* **2007**, *601*, 3268-3275.
(27) Bobrov, K.; Guillemot, L. *Surf. Sci.* **2013**, *611*, 32-39.
(28) Silva, S. L.; Lemor, R. M.; Leibsle, F. M. *Surf. Sci.* **1999**, *421*, 135-145.
(29) Jones, A. H.; Poulston, S.; Bennett, R. A.; Bowker, M. *Surf. Sci.* **1997**, *380*, 31-44.
(30) Leibsle, F. M.; Francis, S. M.; Haq, S.; Bowker, M. *Surf. Sci.* **1994**, *318*, 46-60.
(31) Francis, S. M.; Leibsle, F. M.; Haq, S.; Xiang, N.; Bowker, M. *Surf. Sci.* **1994**, *315*, 284-292.
(32) Bennett, R. A.; Poulston, S.; Bowker, M. *J. Chem. Phys.* **1998**, *108*, 6916-6922.
(33) Okawa, Y.; Tanaka, K.-i. *Surf. Sci.* **1995**, *344*, L1207-L1212.
(34) Poulain, C.; Budinská, Z.; Wiame, F.; Maurice, V.; Marcus, P. *Surf. Sci.* **2017**, *655*, 49-54.
(35) Ruan, L.; Besenbacher, F.; Stensgaard, I.; Laegsgaard, E. *Phys. Rev. Lett.* **1992**, *69*, 3523-3526.
(36) Cho, K.; Kishimoto, J.; Hashizume, T.; Pickering, H. W.; Sakurai, T. *Appl. Surf. Sci.* **1995**, *87-88*, 380-385.
(37) Wintterlin, J.; Volkening, S.; Janssens, T. V. W.; Zambelli, T.; Ertl, G. *Science* **1997**, *278*, 1931-1934.
(38) Germer, T. A.; Ho, W. *Chem. Phys. Lett.* **1989**, *163*, 449-454.
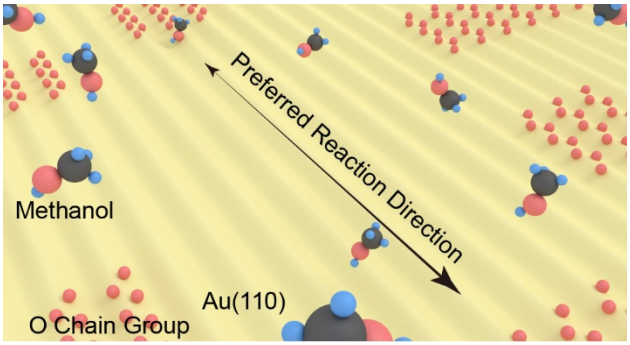
For Table of Contents Only